

# Electrochemical Safeguards Measurement Technology Development at LANL

LA-UR-20-25781

Mark Croce<sup>1</sup>, Daniela Henzlova<sup>1</sup>, Howard Menlove<sup>1</sup>, Daniel Becker<sup>2,3</sup>, Joel Ullom<sup>2,3</sup>

<sup>1</sup>Los Alamos National Laboratory, Los Alamos, NM, USA

<sup>2</sup>University of Colorado, Boulder, CO, USA

<sup>3</sup>National Institute of Standards and Technology, Boulder, CO, USA

## Abstract

As part of the U. S. Department of Energy Office of Nuclear Energy MPACT campaign Virtual Facility Distributed Test Bed, Los Alamos National Laboratory has developed advanced nondestructive assay (NDA) technologies based on gamma ray and neutron signatures. This paper focuses on the development of ultra-high resolution microcalorimeter gamma spectroscopy and the High Dose Neutron Detector (HDND) and their performance evaluation in relation to key measurement points within the Virtual Facility Distributed Test Bed flowsheet. Gamma ray spectroscopy and correlated neutron counting are cornerstones of nuclear material assay for safeguards and security. Advanced nuclear fuel cycles that utilize technologies such as electrochemical separation of spent nuclear fuel (SNF) present new measurement challenges and call for the development of new solutions. The development of microcalorimeter gamma spectroscopy is intended to provide nondestructive isotopic analysis capabilities with sufficient precision and accuracy to reduce the need for sampling and destructive analysis (DA) to meet safeguards and security goals. With nearly 10 times better energy resolution than high-purity germanium detectors, ultra-high-resolution microcalorimeter gamma ray spectrometers have been shown to overcome important uncertainty limits for nondestructive isotopic analysis. Recent development has led to the first microcalorimeter spectrometers designed for use in nuclear facilities and analytical laboratories, including SOFIA (Spectrometer Optimized for Facility Integrated Applications). Implemented in an on-site analytical laboratory, SOFIA could enable precise measurement of the isotopic composition of process samples in a much more rapid and cost-effective manner than destructive analysis. Daily nondestructive measurements to determine changes in key isotopic ratios with 1% 1-sigma precision for input fuel, ER salt, and U/TRU product are feasible with the current instrument. Relative to planar HPGe detectors, SOFIA can significantly improve confidence in results and reduce potential measurement bias by resolving closely spaced gamma ray peaks. The development of the HDND enables the capability to perform neutron counting and NDA in high gamma backgrounds and high count rate applications such as measurements of U/TRU products. The HDND is shown to be capable of tolerating increases in gamma dose rate by almost two orders of magnitude (up to 800 R/hr) with only ~30% reduction in neutron detection efficiency. To demonstrate the HDND performance for U/TRU product accountancy, the instrument was tested with high-mass Pu-bearing U/TRU surrogate materials and demonstrated the capability to measure multiplication using correlated neutron counting. Additionally, the HDND provides a dual capability of neutron and gamma detection for simultaneous neutron counting and gamma-dose measurements and is shown to be a versatile tool for process monitoring applications. By leveraging these and other advanced measurement

technologies for electrochemical facilities, development of a robust and economic safeguards approach will be an important enabling capability for the next generation of nuclear energy.

## Introduction

The Materials Protection, Accounting, and Control Technologies (MPACT) campaign, within the U. S. Department of Energy Office of Nuclear Energy, has developed a Virtual Facility Distributed Test Bed capability for safeguards and security design in future nuclear fuel cycle facilities.<sup>1</sup> This work includes development of next-generation measurement technologies designed to improve the ability to meet requirements in a cost-effective, timely manner with minimal impact on facility operations. Los Alamos National Laboratory has focused on development of advanced NDA technologies based on gamma ray and neutron signatures. Gamma ray spectroscopy and correlated neutron counting are cornerstones of nuclear material assay for safeguards and security.<sup>2</sup> Process modeling and experience in electrochemical separations of SNF show that gamma ray and neutron signatures provide valuable information throughout the Virtual Facility Distributed Test Bed flowsheet (Figure 1).

The complex mixtures of fission products, uranium, and transuranic elements like Pu, Am, and Cm at key measurement points in the facility make isotopic analysis using conventional gamma spectroscopy very challenging. Closely-spaced or overlapping energy peaks and high Compton scattering background observed in high-purity germanium detector (HPGe) spectra lead to excessive measurement uncertainty such that sampling and destructive analysis is required to meet uncertainty target values. This motivates development of an ultra-high resolution gamma spectroscopy technology: microcalorimetry. Microcalorimeters use sensitive low-temperature detectors to measure the thermalized energy of individual gamma rays with energy resolution approximately an order of magnitude better than HPGe. This increased energy resolution has been shown to reduce limiting uncertainty components in Pu isotopic analysis<sup>3</sup> and has motivated development under the MPACT program of a high-throughput architecture and the SOFIA instrument. SOFIA (Spectrometer Optimized for Facility Integrated Applications) is the first microcalorimeter gamma spectrometer designed for deployment in nuclear facilities and analytical laboratories and overcomes many practical limitations of previous systems. The performance of SOFIA was evaluated with samples representative of key measurement points in the facility flowsheet including input accountancy, electrorefiner salt, and uranium/transuranic (U/TRU) products.

From the neutron monitoring perspective, the key neutron signatures in an electrochemical processing facility will be concentrated in the U/TRU product, where the majority of Pu will be contained. The U/TRU product represents a high-density metal material containing uranium, plutonium, and other transuranic (TRU) elements. The actual mass and size of the U/TRU product will likely be driven by processing factors and a safeguards & security by design effort, and could range from several ingots per assembly up to a reduction of a full assembly into a single ingot. In all cases, due to its characteristics (metal, high in Pu and TRU) it will exhibit very high neutron output. The development of an adequate assay and analysis technique for this U/TRU product, therefore, represents one of the key safeguards concerns for an electrochemical processing facility to ensure accountability of the Pu. It is expected that most other streams within the facility will be low in neutron output, however, to ensure adequate safeguards, it will be important to perform

neutron monitoring to detect potential material diversion. This includes the U product, various waste streams such as fission products, metal wastes and overall process monitoring. To address this need, a High Dose Neutron Detector (HDND) was developed specifically for the challenges electrochemical processing applications.

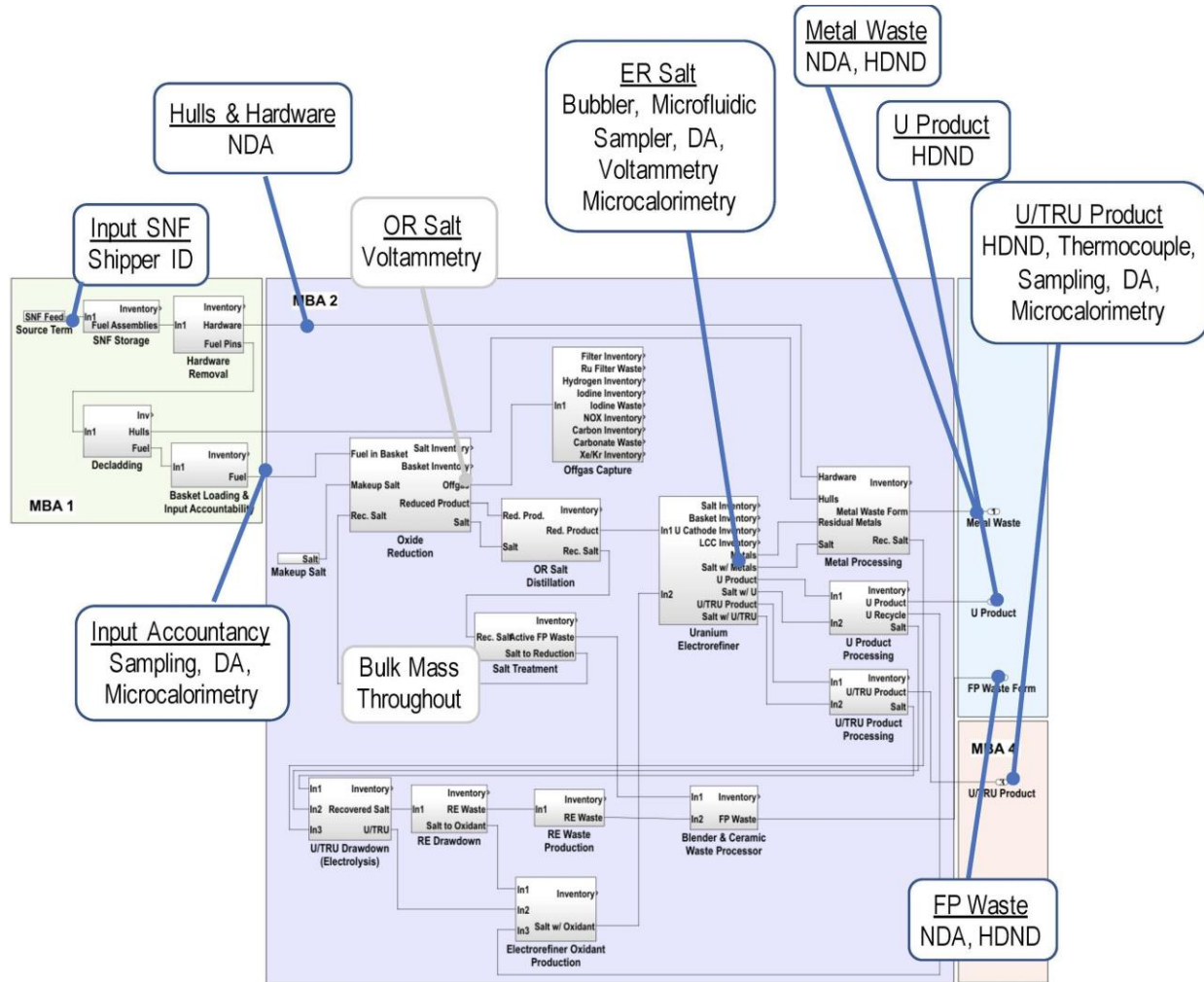


Figure 1. Virtual Facility Distributed Testbed Flowsheet indicating key measurement points for each technology. Microcalorimetry was evaluated for input accountancy, electrorefiner (ER) salt, and uranium/transuranic (U/TRU) products. The High Dose Neutron Detector (HDND) was evaluated for uranium products, U/TRU products, fission product (FP) waste, and metal waste.

## Microcalorimeter Instrumentation Development

Ultra-high resolution microcalorimeter spectroscopy has been shown to reduce important uncertainty terms in gamma-ray isotopic analysis since early stages of development.<sup>3</sup> Energy resolution as good as 22 eV FWHM at 129 keV has been demonstrated,<sup>4</sup> compared with ~550 eV FWHM for a high-quality planar germanium detector. Several key advances in microcalorimeter technology are now enabling a next generation of practical gamma-ray spectrometers designed for use in analytical laboratories and nuclear facilities.<sup>5,6,7</sup> These advances include a high-throughput instrument architecture based on hundreds of individual sensor elements (“pixels”) using microwave frequency-division multiplexing, optimized cryogen-free systems with reduced infrastructure requirements, and automated data processing software.

Successful application of a microcalorimeter gamma spectrometer to advanced nuclear fuel cycle facilities such as an electrochemical processing facility requires the following performance metrics. An energy range of approximately 30-210 keV covers actinide K X-rays and the highest-intensity gamma rays from the most important actinides (U-234 through 238, Np-237 and 239, Pu-238 through 244, Am-241 and 243, Cm-242 and 244). Many fission products can be quantified in this energy range as well. Energy resolution better than 100 eV FWHM at 100 keV (approximately 5 times better than planar HPGe detectors) is sufficient to resolve important peak overlaps such as the 104.23 keV <sup>240</sup>Pu gamma ray and the 103.73 keV Pu K $\alpha$ 1 x-ray. In an electrochemical processing facility, large quantities of material and high activity levels are available for in-situ nondestructive measurements. This requires an instrument with high count rate capability. If samples are taken, they are often very small quantities suitable for safe handling in an analytical laboratory. This requires an instrument with high detection efficiency. High count rate capability and high detection efficiency are both enabled by microcalorimeter instruments with hundreds of individual sensor elements.

The following requirements are equally important. A microcalorimeter spectrometer must be compatible with the utilities and space available in a facility or analytical laboratory and comply with applicable regulations. It must be suitable for measuring a variety of materials and item geometries. It must be easy to use and provide reliable and stable operation with minimal maintenance. The goal of SOFIA is to create a high-throughput instrument to meet these requirements by leveraging recent technology developments. SOFIA (Figure 2) overcomes many practical limitations of previous microcalorimeter instruments and is suitable for operation in nearly any facility worldwide.

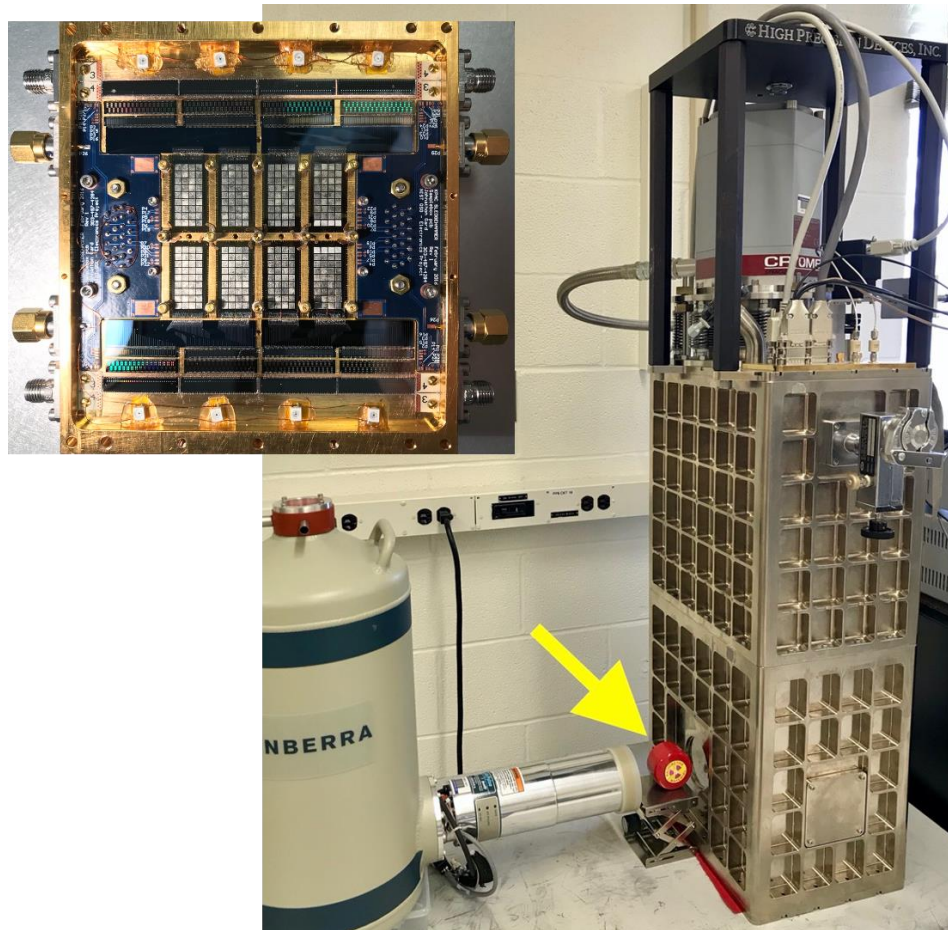


Figure 2. The SOFIA microcalorimeter gamma spectrometer is designed for deployment in nuclear facilities and analytical laboratories with a compact tabletop cryostat (right) that uses no liquid cryogens. Samples (indicated by the arrow) are placed outside the instrument, or the instrument can be moved next to a hot cell port or glovebox. The 256-pixel microcalorimeter array (inset) provides typical energy resolution of 60-70 eV FWHM at 129 keV and is capable of count rates exceeding 5000 per second. A planar germanium detector (energy resolution  $\sim$ 550 eV FWHM at 129 keV) is shown on the left for comparison.

One of the main goals in developing SOFIA was to reduce the infrastructure required to operate a microcalorimeter system. The High Precision Devices Model 102 (along with the STAR Cryoelectronics DRC-100 which is derived from the same NIST design) is the smallest commercially-available cryostat capable of reaching the detector operating temperature of 80 mK. The standard version of this cryostat uses a Cryomech PT407 pulse tube refrigerator that requires three-phase 200/230V (7.0 kW) electrical power and chilled water. The chilled water and three-phase power requirements are difficult to meet in many facilities. For SOFIA, the PT407 was replaced with a PT403 pulse tube that requires only single-phase 208-230V power (3 kW). The PT403 has a similar form factor and only minor mechanical modifications were required for installation. No cooling water is required, because it uses an air-cooled compressor. The power requirement is similar to that of a large window air conditioner. An adiabatic demagnetization refrigerator provides reliable operation at the 90 mK detector operating temperature for

approximately 24 hours following a 2-hour regeneration cycle. No liquid cryogenics or He-3 are used in the system.

SOFIA has demonstrated energy resolution as good as 59 eV FWHM at 97 keV. The detector array is mounted behind a side-looking window to enable a wide variety of measurement configurations. Samples are placed next to the cryostat, or the instrument can be easily relocated next to a hot cell port or glove box for in-line measurements. The internal design of SOFIA minimizes the distance from the window to the detector array in order to maximize detection efficiency for small samples placed against the detector window. Conversely, high count rate capability is needed when measuring high-activity samples. As with germanium detectors, energy resolution degrades at high count rates. For a specific application, the count rate and associated statistical uncertainty for a given measurement time is balanced with the energy resolution and associated systematic uncertainty. SOFIA has been tested to yield 100 eV FWHM energy resolution at approximately 20 counts per second per pixel. With the full 256-pixel array, this corresponds to 5120 counts per second and approaches count rates typical of germanium detectors. A rate of approximately 10-20 counts per second per pixel is an appropriate balance between high throughput and energy resolution for most measurements.

Software for data processing and isotopic analysis is needed for practical application of microcalorimeter spectrometers.<sup>8,9</sup> Robust, completely automated software was developed (Figure 3) to process raw data from individual microcalorimeter pixels into a single spectrum as required for subsequent analysis. Individual pulse records from every pixel are saved to disk and processed after acquisition. Software for real-time processing and live spectral display is under development.

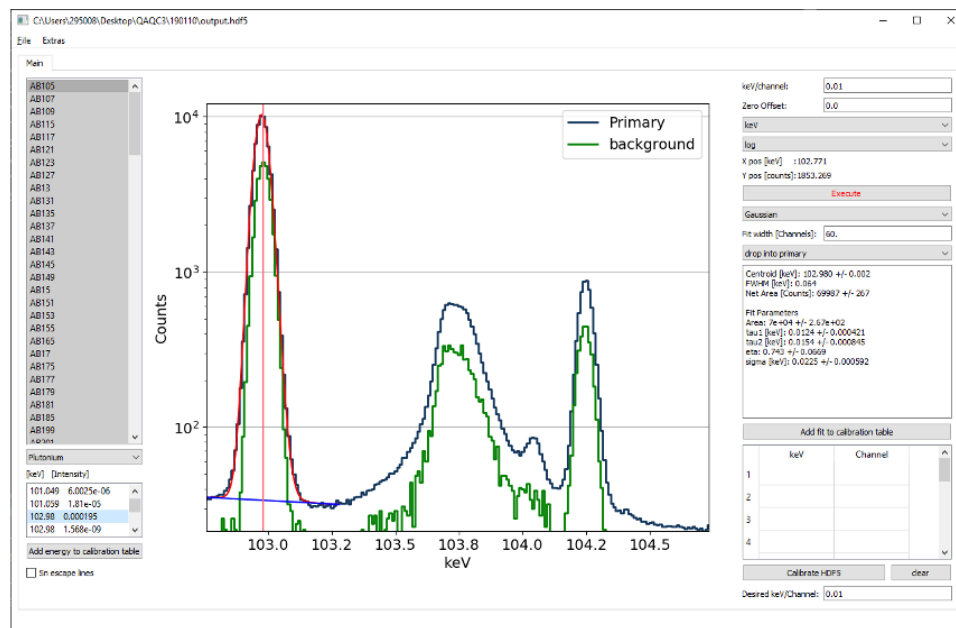


Figure 3. A graphical user interface enables rapid energy calibration and verification of data quality after automated processing of pulse data from each individual microcalorimeter pixel into a single energy spectrum.

Arrays of hundreds of microcalorimeter pixels are required to achieve useful count rates and detection efficiency because individual pixels are small ( $\sim 1 \text{ mm}^2$ ) and slow ( $\sim 10^{-3} \text{ s}$ ) compared to

semiconductor detectors. Each pixel in a microcalorimeter array acts as an independent spectrometer and thus adds to the total detector volume and count rate of the instrument. Technology development under DOE NE's University Program (NEUP) focused on advancing the performance potential of microcalorimeter arrays for gamma spectroscopy and was key to the development of SOFIA. This NEUP work is so tightly coupled to LANL's MPACT effort that it is described here rather than in the manuscript describing other NEUP programs in this same issue.<sup>10</sup>

## NEUP Technology Development

The first thrust of the NEUP research was to develop microwave frequency-domain multiplexing (mumux) techniques that allow many microcalorimeter sensors to be measured using a single amplifier, a key enabling technology for large arrays. For sensors operated at millikelvin temperatures, it is impractical to have separate electrical connections and readout amplification for each sensor in an array because of the thermal load and mechanical complexity of such a scheme. In microwave multiplexing, each microcalorimeter pixel modulates a dedicated thin-film microwave resonator, and all the resonators are coupled to a common microwave feedline. A sum of microwave tones is injected at one end of the feedline and measured at the other end by a single shared semiconductor amplifier at the 4 K stage of the cryostat. The frequency of each tone is tuned to one of the microwave resonators. Electronics at room temperature synthesize the input tones and also digitize, channelize, and demodulate the output tones to extract the sensor signals. During this work, multiplexing components as well as arrays of superconducting transition-edge sensor microcalorimeters were designed and fabricated. Figure 2 (inset) shows the detector assembly with SMA microwave connectors at each corner, multiplexing chips in rows at the top and bottom, and eight TES microcalorimeter chips in the center. Software and firmware were developed for open-source ROACH2 electronics<sup>11</sup> to perform the microwave tone manipulation. Details of this work appear in preceding publications.<sup>5,6,7</sup>

The net impact of mumux is the ability to build microcalorimeter instruments with more pixels, faster pixels, and more stable performance than was previously possible. Two instruments were developed for MPACT, called SLEDGEHAMMER and SOFIA, in order to assess the analytical value of microcalorimeters for nuclear materials accounting. SLEDGEHAMMER was the first microcalorimeter instrument to use microwave readout and it is based on a 250 pixel array similar to that in Figure 2. SOFIA uses a similar detector package to SLEDGEHAMMER. An instrument based on this scalable architecture with close to 500 pixels is presently under development for the analytical laboratory at Idaho National Laboratory.

The second NEUP thrust focused on quantitative isotopic analysis. Software was developed for the analysis of Pu mixtures and is now being adapted to analyze U/TRU materials. This software, called SAPPY (Spectral Analysis Program in PYthon), builds on LANL spectral analysis software and provides a flexible response-function analysis framework with rigorous uncertainty analysis. SAPPY fits peak areas and computes a relative efficiency curve to determine isotopic ratios in an approach similar to the widely-used FRAM software.<sup>12</sup> In contrast to FRAM, SAPPY provides improved peak fitting options and expanded uncertainty analysis such as the ability to include uncertainty in gamma ray energies or x-ray linewidths. The building blocks and algorithms in this software can likely be adapted to a wide range of analytical tasks. An important goal that has been

successfully achieved is that the same software can be used for both microcalorimeter and germanium data. This allows analytical results from the two detector technologies to be compared with confidence that any differences are not caused by the use of different reference data or different treatment of statistical error terms. For high statistics spectra, the errors in the reported isotopic ratios can be dominated by uncertainties in the tabulated branching ratios, an effect observed previously in reference 3. As a result, microcalorimeter spectra from well characterized reference materials have been recently used to produce improved values for many gamma-ray branching ratios.<sup>13</sup> Figure 4 shows an example of the results from measurement of a Pu sample. SAPPY can be readily adapted to different measurement scenarios since peak area determination and source-detector efficiency curve determination are nearly universal tasks. SAPPY can be extended to uranium enrichment measurements in the near future.

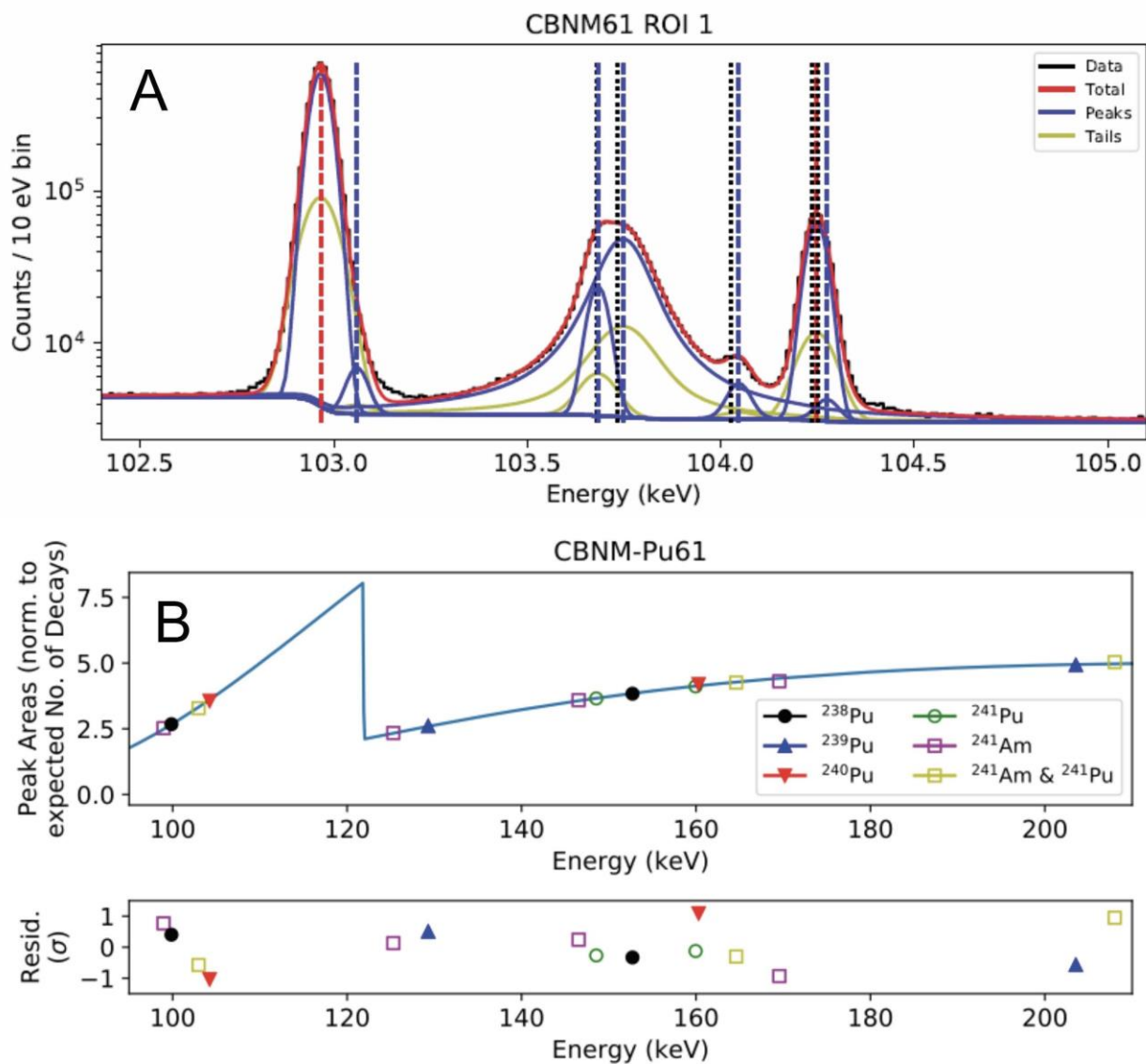


Figure 4A. Data (black) and fit (red) for spectral ROI centered on 103.5 keV from a Pu sample. Black vertical dotted lines show tabulated peak positions. Red vertical dashed lines show fit peak

positions for peaks used in isotopic analysis. Blue vertical dashed lines show fit peak positions for nuisance peaks. Each spectral feature is composed of a primary curve (blue) and a tail (yellow) to account for non-Gaussian behavior of the detector response function. Figure 4B shows the result of fitting for source-detector efficiency curve and isotopic ratios. Colored markers correspond to individual gamma-ray lines where each isotope has a particular color. Lines whose intensity is consistent with the extracted efficiency curve (blue) fall on the curve. The fit residuals shown in the bottom panel are well clustered around zero.

## **Microcalorimeter Measurement Performance**

Precision isotopic analysis by nondestructive gamma spectroscopy has many advantages for electrochemical processing facility safeguards. Compared to sampling and destructive analysis, rapid NDA has a minimal impact on facility operations and a much lower cost per measurement. This makes it possible to complete more individual measurements in order to reduce the effect of sampling error and improve timeliness of detection of material diversion. This section details quantitative analysis of the SOFIA microcalorimeter gamma spectrometer capabilities for the key measurement points of input accountancy, electrorefiner (ER) salt, and uranium/transuranic (U/TRU) products.

### ***Input Accountancy***

Input accountancy of solid fuel has been identified as one of the main measurement challenges in the facility flowsheet. Verifying fissile content and irradiation history of the input SNF is difficult due to the presence of intense fission product activity and intrinsic variability in composition of spent fuel elements due to their position in a reactor. Compared with destructive analysis, nondestructive microcalorimeter gamma spectroscopy can perform many more individual measurements. Therefore, microcalorimetry offers a way to not only reduce the effect of sampling error, but to accurately determine the distribution of the composition of solid form spent nuclear fuel. Improved energy resolution compared to HPGe can reduce the effect of large Compton scattering background from high-energy fission product gamma rays and more accurately quantify actinide signatures in the presence of neighboring peaks.

Two samples of high-burnup spent fuel representative of material that may be processed by electrochemical separations were measured. These samples were provided by MPACT program collaborators at Pacific Northwest National Laboratory and shipped to Los Alamos for measurements. ATM109 was received as a dried sample of dissolved BWR fuel from the Quad Cities I reactor. This material had an initial enrichment of ~3%, burnup of approximately 67-70 GWd/MTU, and a discharge date of September 1992.<sup>14</sup> The Sister Rod sample was a direct swipe sample of “sister rod” PWR fuel from the North Anna reactor with an initial enrichment of 3.59-4.55 wt%, burnup of approximately 50-58 GWd/MTU, and a discharge date between 1989 and 2011.<sup>15</sup>

Analysis efforts have focused on the 100 keV region which contains peaks from the  $K\alpha_1$  x-ray line of Pu (103.7 keV),  $^{155}\text{Eu}$  (105.3 keV) and  $^{239}\text{Np}$  (106.1 keV).  $^{155}\text{Eu}$  (4.74 y half-life) is a fission product with substantially different chemical behavior from the actinides.  $^{239}\text{Np}$  is produced by the alpha decay of  $^{243}\text{Am}$ . With a half-life of only 2.4 days,  $^{239}\text{Np}$  is in secular equilibrium with  $^{243}\text{Am}$

which is produced by neutron capture reactions and correlates with Pu content in the spent fuel.  $^{239}\text{Np}$  is therefore an excellent indicator of the transuranic content of the fuel, and changes in the  $^{239}\text{Np}$  relative to fission products could signal diversion of Pu. Because these two peaks from  $^{155}\text{Eu}$  and  $^{239}\text{Np}$  are so close together, their heights can be compared to infer relative quantities or changes in the amounts of these two nuclides with little uncertainty introduced from the source-detector efficiency curve. Microcalorimeter and HPGe spectra in this energy region are shown in Figure 5. The microcalorimeter data easily resolves the two peaks of interest in both samples, while the HPGe data barely resolves the peaks in the ATM109 sample and not at all in the Sister Rod sample. Systematic uncertainty has the potential to be significant in analysis of HPGe data due to peak overlaps. The improved resolution of the microcalorimeter data, where peaks are well-resolved from each other, nearly eliminates this type of uncertainty contribution and therefore allows peaks in this region to be confidently used for quantitative analysis. The following analysis considers statistical uncertainty achievable with microcalorimeter data as this is anticipated to be the primary contribution to total measurement uncertainty for microcalorimeter measurements of input fuel.

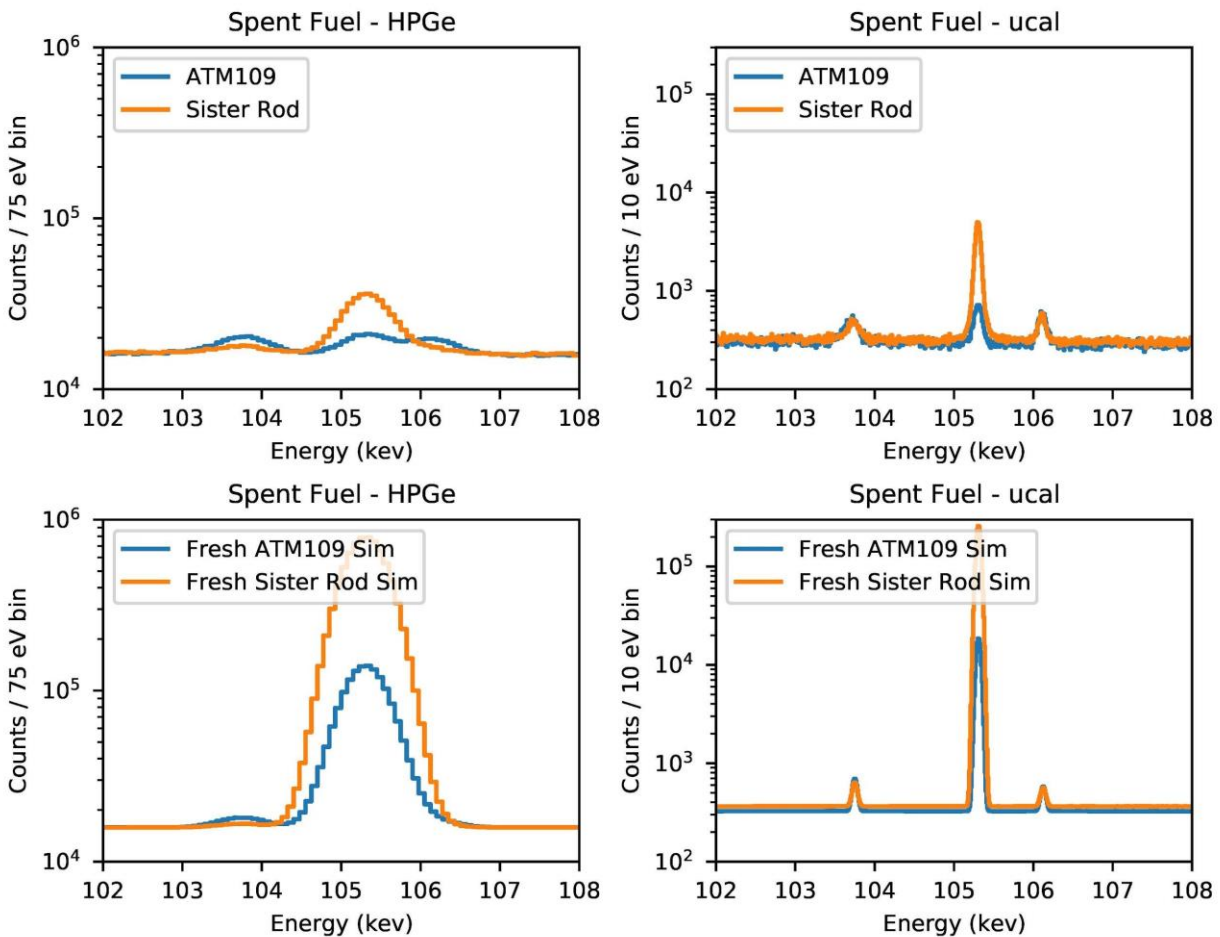


Figure 5. Top: Measured microcalorimeter and HPGe spectra for spent fuel samples. Bottom: Simulated spectra for “Fresh” spent fuel samples, described in the text.

To determine the number of counts required in order to obtain 1% precision in the relative peak areas Monte Carlo simulations based on the measured spectra were performed. Model spectra were

used for the samples as measured in Figure 4, and with model spectra representing the samples a short time after discharge from the reactor. The latter spectra were produced by starting with the recent measurements and making two changes: increasing the height of the  $^{155}\text{Eu}$  peak relative to the  $^{239}\text{Np}$  peak by a factor of  $\sim 80$  to account for the decay of  $^{155}\text{Eu}$  over 27 - 30 years, and increasing the level of background by a factor of 2 to account for Compton scattering from  $^{137}\text{Cs}$  (30 y half-life). For each model spectrum, 10,000 iterations of the spectrum were produced to account for Poisson statistics, and a curve fitting routine was applied to determine the average value and standard deviation of the ratio of the  $^{155}\text{Eu}$  to  $^{239}\text{Np}$  peak areas.

Table 1 shows the analysis results expressed as the number of counts required to achieve 1-sigma uncertainties of 1 %, 3 %, and 5 % in the areas of each of these peaks. Turning these relative numbers of required counts in the 105.3 keV peak into relative acquisition times requires balancing energy resolution, detection efficiency, and total count rates. Microcalorimeter systems are rapidly advancing in count rate capability and are approaching count rates achieved with HPGe detectors. HPGe detectors also measure photons at much higher energies than microcalorimeters. This is an advantage for some applications but is a disadvantage in a case like this where the lines of interest appear at low energies, and high-energy photons contribute to dead time without improving the analysis. For the Sister Rod sample, approximately 0.26 % of the total counts are in the 105.3 keV peak. This implies that 19e6 total counts would be required to achieve 1-sigma uncertainty of 1 % in the 105.3 keV peak area, and 83e6 total counts for 1-sigma uncertainty of 1 % in the 106.1 keV peak area. For SOFIA operating at 5,000 counts per second, meeting these criteria would require 1 hour and 4.6 hours respectively. This is a good match for daily measurements of the input fuel in an electrochemical processing facility. As the speed of individual microcalorimeters and the size of microcalorimeter arrays improve, shorter counting times will be possible. A similar analysis of the Sister Rod spectrum for an HPGe detector with 700 eV FWHM resolution indicates that to achieve the same statistical uncertainty, a factor of 16 more counts are required. For a count rate of 10,000 per second, the HPGe detector would require 1.5 days of measurement time for 1-sigma statistical uncertainty of 1% on the 106.1 keV peak area.

Sample	105.3 / 106.1 Peak Area Ratio	105.3 keV Counts for Given 1-sigma Uncertainty in 105.3 keV Peak Area			106.1 keV Counts for Given 1-sigma Uncertainty in 106.1 keV Peak Area		
		1 %	3 %	5 %	1 %	3 %	5 %
Sister Rod	15.7	11e3	1.2e3	0.45e3	23.3e3	2.5e3	0.93e3
Simulated "Fresh" Sister Rod	1300	9.6e3	1.1e3	0.38e3	38.5e3	4.3e3	1.55e3
ATM109	1.32	17.5e3	2.0e3	0.70e3	19.5e3	2.18e3	0.78e3
Simulated "Fresh" ATM 109	71	10.0e3	1.13e3	0.40e3	32.8e3	3.6e3	1.3e3

Table 1. Counts required by microcalorimeter detectors to achieve 1-sigma uncertainties of 1 %, 3 %, and 5 % uncertainty in peak areas for the  $^{155}\text{Eu}$  and  $^{239}\text{Np}$  peaks.

*Electrorefiner Salt*

Much of the fissile material inventory in an electrochemical processing facility is contained within the electrorefiner salt, which makes the electrorefiner one of the most important measurement points for safeguards. Multiple NDA measurements are desirable to address sampling error because ER salts may contain fine particles dispersed through the salt, dross on the top layer, and insoluble debris on the bottom of the vessel.

Two samples of electrorefiner (ER) salt used in spent nuclear fuel separation were provided by MPACT program collaborators at Idaho National Laboratory and sent to Los Alamos for measurements. The two salt samples were collected after electrorefiner operation with two different input material compositions. As with input fuel, intense fission product activity in the electrorefiner salt makes it challenging to resolve actinide signatures. However, it is very clear that the actinide composition is different between the samples. The 100 keV region (Figure 6) shows gamma ray peaks from  $^{155}\text{Eu}$  and  $^{239}\text{Np}$  as well as intense Pu X-rays understood to result from the decay of transuranic nuclides. A Monte Carlo approach similar to that in the previous section was applied to determine the number of counts required for 1-sigma uncertainty of 1%, 3%, and 5% on the 105.3 keV ( $^{155}\text{Eu}$ ) and 106.1 keV ( $^{239}\text{Np}$ ) peaks. Table 2 summarizes results. The measured spectrum for sample 482 had a total of 9M counts and is the most challenging case with 0.061% in the 105.3 keV peak and 0.014% in the 106.1 keV peak. For SOFIA counting at 5000 counts per second, this implies that 1-sigma uncertainty of 1% would be achieved in 2.1 hours for the 105.3 keV peak and 24.4 hours for the 106.1 keV peak. For sample 582, 1-sigma uncertainty requires only 2.4 and 1.6 hours respectively.

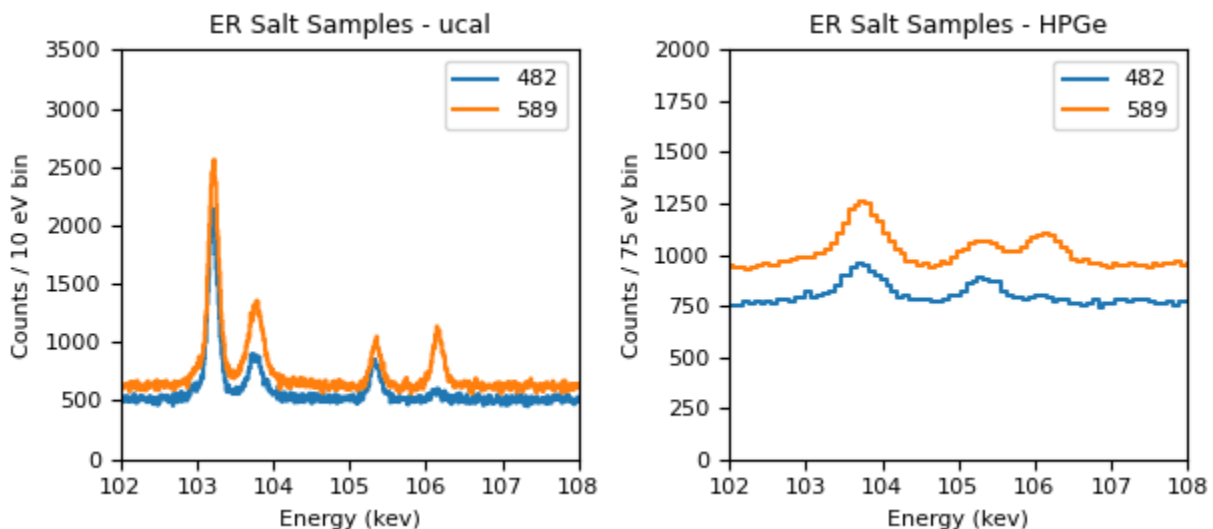


Figure 6. Microcalorimeter (left) and HPGe (right) spectra, for two different ER salt samples. The strong peak at 103.2 keV in the microcalorimeter spectra is from  $^{153}\text{Gd}$ , which was used to aid calibration. The 106.1 keV peak from  $^{239}\text{Np}$  is much better resolved above background in the microcalorimeter spectra.

Sample	105.3 / 106.1 Peak Area Ratio	105.3 keV Counts for Given 1-sigma Uncertainty in 105.3 keV Peak Area			106.1 keV Counts for Given 1-sigma Uncertainty in 106.1 keV Peak Area		
		1 %	3 %	5 %	1 %	3 %	5 %
ER Salt Sample 482	4.4	22.6e3	2.5e3	0.90e3	60.6e3	6.7e3	2.4e3
ER Salt Sample 589	0.79	23.4e3	2.6e3	0.94e3	21.0e3	2.3e3	0.84e3

Table 2. Counts required by microcalorimeter detectors to achieve 1-sigma uncertainties of 1 %, 3 %, and 5 % uncertainty in peak areas for the  $^{155}\text{Eu}$  and  $^{239}\text{Np}$  peaks.

### *Uranium/Transuranic (U/TRU) Products*

U/TRU ingots contain the majority of the plutonium and other transuranic elements from the process along with a large fraction of uranium which motivates application of precision nondestructive isotopic analysis techniques for accountancy. To address this challenge, a high-burnup CBNM61 plutonium reference material and a 2.95% enriched uranium standard were measured and the data was combined to produce a simulated spectrum corresponding to an item with 50% plutonium and 50% uranium by mass. The component spectra were scaled according to the relative heights of the  $^{239}\text{Pu}$  peak at 203.55 keV and the  $^{235}\text{U}$  peak at 205.3 keV, the tabulated values for the half-lives of these isotopes, and the known Pu and U content of the two samples. This approach assumes identical efficiency curves for the two measurements. While the efficiency curves are known to differ depending on the sample form and packaging, this simplified approach is a useful first approximation of the expected spectrum from a real U/TRU sample. The same procedure was applied to microcalorimeter and HPGe spectra.

Figure 7 shows the resulting synthetic microcalorimeter spectrum, along with the measured CBNM61 Pu spectrum. The synthetic U/TRU spectrum is nearly identical to the CBNM61 spectrum, with a few additional peaks visible from uranium. This demonstrates the feasibility of applying the isotopic analysis software (SAPPY) to determine an efficiency curve and Pu isotope ratios. The resulting Pu isotope ratios were statistically identical to the ratios extracted from the pure CBNM61 spectrum. The resulting efficiency curve and area of the  $^{235}\text{U}$  185.7 keV peaks were then used to determine the  $^{235}\text{U}/^{239}\text{Pu}$  ratio. For the 185.7 keV peak the answer was 7.5 % higher than the “true” value, with an uncertainty of 2.2%. Given the incorrect assumption of identical efficiency curves in the two measurements, these results are encouraging and suggest the potential of microcalorimetry to accurately extract the  $^{235}\text{U}/^{239}\text{Pu}$  ratio from a U/TRU sample. To assess any advantage microcalorimeters may have over HPGe for extracting  $^{235}\text{U}/^{239}\text{Pu}$  ratios, a synthetic U/TRU spectrum was constructed based on HPGe measurements of the same materials. The resulting synthetic HPGe spectrum is shown in Figure 8. For SOFIA operating at 5,000 counts per second, the  $^{235}\text{U}/^{239}\text{Pu}$  ratio can be measured to a 1-sigma statistical precision of 1.0 % in 24 hours. An HPGe measurement operating at 10,000 counts per second is limited to a 1-sigma statistical precision of 1.8 % in 24 hours. This analysis considers only statistical uncertainty. The improved

energy resolution of the microcalorimeter spectrum also significantly reduces the potential for bias resulting from peak overlaps or interferences, therefore improving confidence in results and reducing the need for complementary destructive analysis. Optimized shielding to attenuate less-relevant low-energy gamma rays such as the 59 keV peak of  $^{241}\text{Am}$  should improve the precision achievable by SOFIA in 24 hours to 0.75 %.

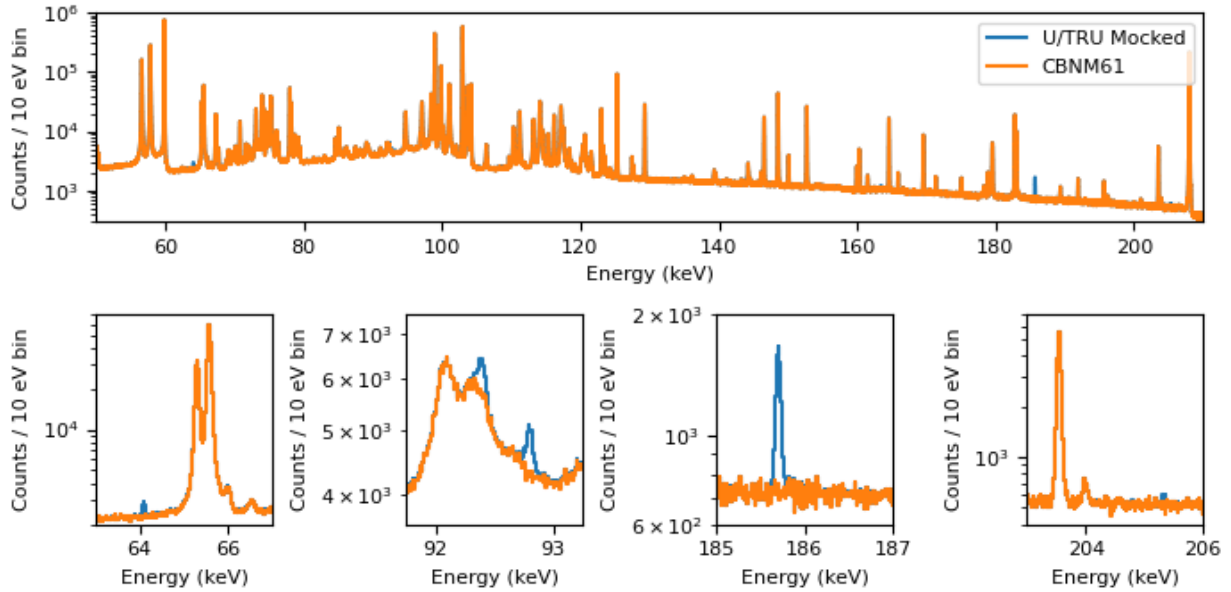


Figure 7. Synthetic U/TRU microcalorimeter spectra made by scaling and combining measured Pu and U reference material spectra. The inset plots zoom in on areas where the differences between the synthetic spectrum and the CBNM61 reference spectrum are clearly visible. From left to right, observed peaks include the 63.3 keV peak of Th-234, the 92.4 and 92.8 keV peak of  $^{234}\text{Th}$  overlapping with Sn-escape peaks from U X-rays at 117 keV, the 185.7 keV peak of  $^{235}\text{U}$ , and the 205.3 keV peak of  $^{235}\text{U}$  (just barely visible).

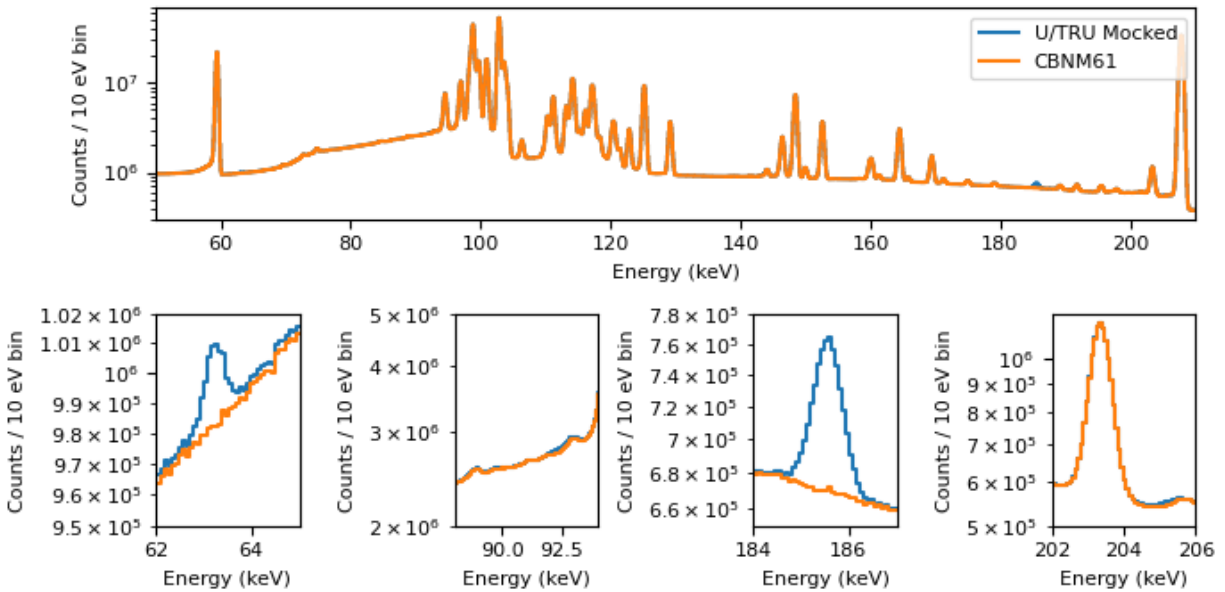


Figure 8. Synthetic U/TRU HPGe spectra made by scaling and combining measured Pu and U reference material spectra. The inset plots show the same areas as in Figure 7.

## High-Dose Neutron Detector (HDND)

To address the need for neutron based non-destructive assay (NDA) technology adequate for the unique challenges of electrochemical processing facilities and to enable NDA measurements of U/TRU products, a novel technology based on boron-lined parallel-plate proportional counters was developed and evaluated as part of the MPACT program. It features high count rate capability to accommodate high neutron emission rates, while exhibiting low sensitivity to gamma-ray backgrounds encountered in electrochemical processing applications. Neutron based non-destructive assay (NDA) systems traditionally in use in current nuclear safeguards applications typically employ fission chambers or  $^3\text{He}$ -based proportional counters. Fission chambers are used in applications where high gamma-ray backgrounds are anticipated, due to their low sensitivity to gamma rays; however, they provide very low detection efficiency on the order of 0.01%.  $^3\text{He}$ -based systems allow for higher detection efficiencies, enabling benefit from the additional information provided by correlated neutron counting;<sup>2</sup> however, at the expense of slow signal rise time characteristics and higher sensitivity to gamma-ray backgrounds. The boron-based detectors have the additional advantage of being nonhazardous with respect to transport and facility regulations.

To address these aspects and target technology specific for high neutron count rate, gamma tolerant application, the boron-lined proportional technology was selected for electrochemical processing measurements. This technology was developed by Precision Data Technology, Inc. (PDT) and is based on boron-lined parallel-plate proportional counters. The benefit of the technology lies in its inherent capability to sustain high count rates, provide sufficient efficiency for correlated counting, and design features that allow minimizing its gamma-ray sensitivity. In addition, the boron-10 coated detector does not utilize  $^3\text{He}$  gas and as such provides a viable detection technology for

<sup>3</sup>He-replacement purposes. The following sections will describe the detector design along with its performance characteristics of interest for the electrochemical processing applications.

## HDND Features

The HDND is based on boron-lined parallel-plate technology developed in collaboration with Proportional Data Technology, Inc. (PDT). The HDND consists of six narrow (~0.5 cm) boron-lined detection plates filled with Ar and CO<sub>2</sub> gas at sub atmospheric pressure interleaved with high density polyethylene (HDPE) moderator. The individual detection plates are hermetically sealed to remove any potential sources of impurities from the counting gas and enable gas purification procedures to assure high system reliability. The sealed-cell concept utilizes corrugated surfaces to increase boron-coated surface area and simultaneously provide additional structural integrity. The internal layout of the HDND was optimized using MCNPX for low gamma-ray sensitivity and high neutron detection efficiency.<sup>16</sup> The outer dimensions of the detector module are 20 cm (w) x 25 cm (h) x 16 cm (d). The height of 25 cm includes a compact electronics junction box. Figure 9 shows a photograph of the HDND detector and its internal layout.

The parallel plate design maximizes the boron surface area, which in combination with optimum amount of HDPE moderating material provides high neutron detection efficiency. As such it provides a viable alternative for traditional <sup>3</sup>He-based technologies. In addition, the narrow parallel-plate spacing along with less than 1 atm pressure Ar and CO<sub>2</sub> gas fill assure the fast timing characteristics of the detector signal. In particular, the narrow gas cells assure limited spread of ionization tracks and the gas fill results in electron drift velocities of several cm/μs.<sup>17</sup> In comparison, the ionization in the traditional 2.54 cm diameter <sup>3</sup>He tubes exhibits a wide range of track distances and electron drift velocities for the nominal (standard) 4 atm gas pressure corresponding to <1 cm/μs.<sup>18,19</sup> The rise-time characteristics of the PDT parallel-plate system thus correspond to tens of nanoseconds compared to several hundred nanoseconds or even as long as 1-2 μs in the case of <sup>3</sup>He tubes. To support high-count rate applications, fast amplifiers were developed by PDT.<sup>20</sup> The HDND signal processing electronics includes 6 fast-amplifiers, which further reduces system dead-time. The individual outputs are recorded in list mode (event-by-event) in addition to total output of the 6 cells. The total output signal is compatible with standard nuclear safeguards instrumentation (i.e. shift register module<sup>2</sup>).

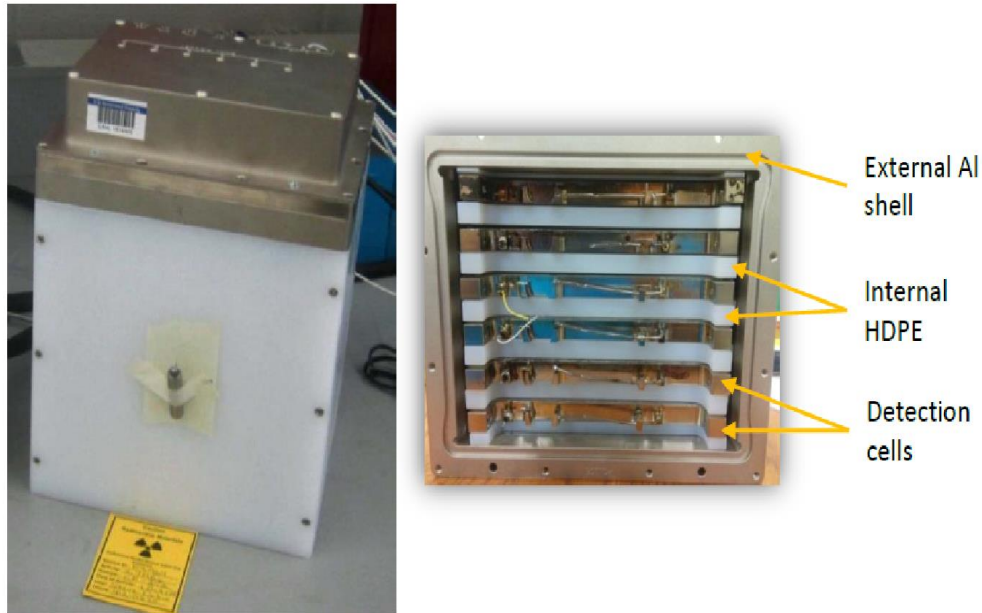


Figure 9. HDND module with  $^{252}\text{Cf}$  source taped to the front face (left); internal layout with 6 sealed detection plates and HDPE layers between individual detection plates (right).

The key features of HDND technology include:

- High neutron count rate capability and broad dynamic range;
- Low and tunable gamma-ray sensitivity;
- Dual detection mode capability (neutron and gamma detection);
- Directionality of motion measurement capability (from multi-plate design);
- Sufficient neutron detection efficiency for correlated counting (in configurations with 2 or more HDND modules)

### **HDND Performance for Electrochemical Facility Applications**

This section provides more details on the individual HDND capabilities of relevance for electrochemical processing applications.

#### ***HDND Performance and Neutron/Gamma Detection Capability***

The HDND was tested under different gamma dose rates ranging from 50 R/h up to 800 R/h. The high dose tests were performed at the LANL Radiation Instrumentation Calibration Facility using 1000 Ci  $^{137}\text{Cs}$  source. The results of this evaluation were described in more detail in reference 21 and highlighted the key feature of HDND, which is its capability to operate in high gamma dose rates with only a small reduction of neutron detection characteristics. This is illustrated in Figure 10, which shows high voltage curve characteristics of the HDND for a neutron source ( $^{252}\text{Cf}$ ) compared to several different gamma dose rates from  $^{137}\text{Cs}$  at different distances from the HDND surface. The neutron count rate increases only very slightly with high voltage (HV) resulting in a gradual plateau, which is typical for boron-lined proportional counters. Contrary to that, the gamma pile-up results in a steep increase in count rate with increasing HV. Furthermore, the onset

of gamma pile-up shifts towards lower HV settings with increasing gamma dose rate, thus reducing neutron detection efficiency. However, even for almost two orders of magnitude increase in gamma dose rate (50 to 795 R/hr), the neutron count rate decreases only by about 30%. This demonstrates that HDND can tolerate a broad range of gamma dose rates with only moderate change in neutron detection performance.

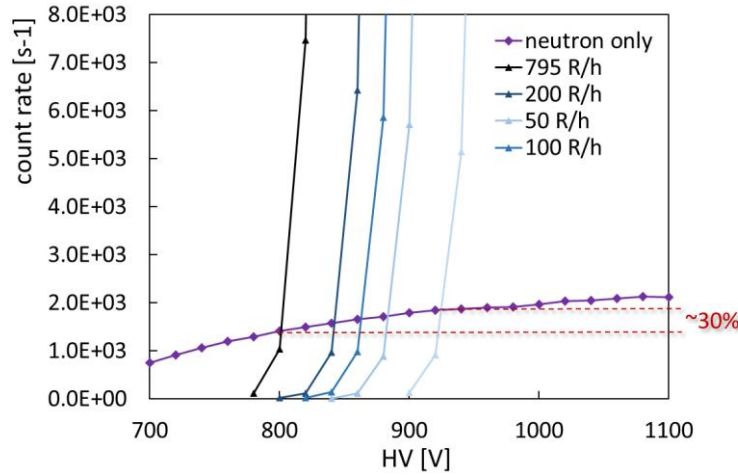


Figure 10. HDND neutron detection performance in a high gamma dose environment.

In addition, the high gamma dose measurements provided key insight into some advanced analysis capabilities that can be employed with the HDND. In particular, the capability to simultaneously evaluate gamma dose rate while performing regular neutron assay is useful. The analysis utilizes distinctly different HV curve characteristics of neutron and gamma-induced signals illustrated in Figure 10 for  $^{137}\text{Cs}$  and  $^{252}\text{Cf}$  sources; gamma pile-up results in a steep increase in count rate with increasing HV, while the neutron HV characteristics in the plateau region remain relatively unchanged. The gamma measurement concept will therefore use a short measurement at increased HV setting ( $\sim 80\text{V}$  above the standard neutron operating HV) to extract gamma-induced count rate (the neutron contribution will be negligible) that can be related to gamma dose rate using a prior calibration.

This concept was evaluated using a pair of  $^{137}\text{Cs}$  sources placed at an increasing distance from the HDND front face to vary the gamma dose rate. Measurements were performed at an operating HV of 1000V, where negligible gamma signal was detected for all dose rates and at elevated HV of  $+80\text{V}$  (i.e. 1080V) to record the gamma-induced count rate. The results are shown in Figure 11 and illustrate an increasing trend of the gamma count rate with the dose rate. Such concepts could be easily implemented in practical measurements, where the HDND HV would be increased by  $\sim +80\text{V}$  relative to operating HV used for neutron measurements, to extract the gamma count rate. Note that changing HV is straightforward using HDND standard electronics, and for practical applications it can be incorporated in a dedicated software.

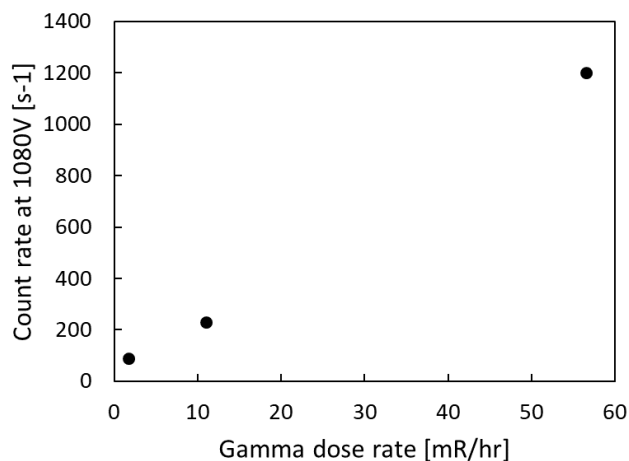


Figure 11. HDND count rate measured at an elevated HV setting of 1080V as a function of  $^{137}\text{Cs}$  dose rate.

### *Process Monitoring*

Another important aspect of HDND for use in electrochemical processing applications is its process monitoring capability. To demonstrate this capability, measurements with  $^{252}\text{Cf}$  and  $^{137}\text{Cs}$  sources were performed using the LANL rail system, which allows controlled linear motion at a range of speeds. Photographs of the experimental configuration are shown in Figure 12.

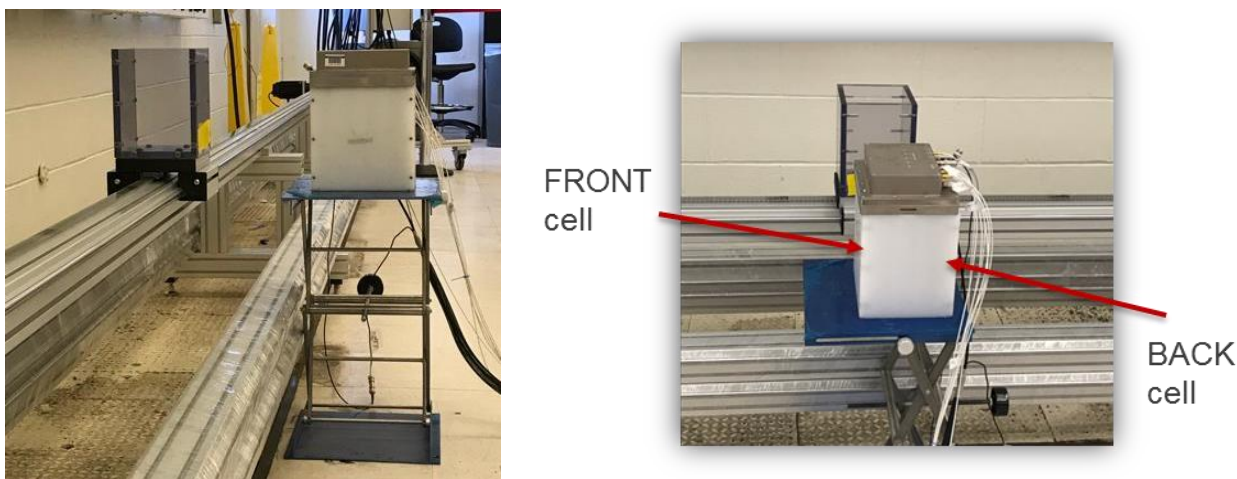


Figure 12. HDND configuration during moving source measurements; (left) HDND positioned sideways with respect to acrylic sample holder, (right) front view of the configuration to illustrate back and front HDND cell ordering.

Each of the  $^{252}\text{Cf}$  or  $^{137}\text{Cs}$  sources, attached to the acrylic sample holder, was moved in the direction from front to back past the HDND side. A series of measurements with sample holder speeds

ranging from 1 to 10 cm/s were performed and the results of these measurements are summarized in Figure 13 for neutron (top) and gamma sources (bottom).

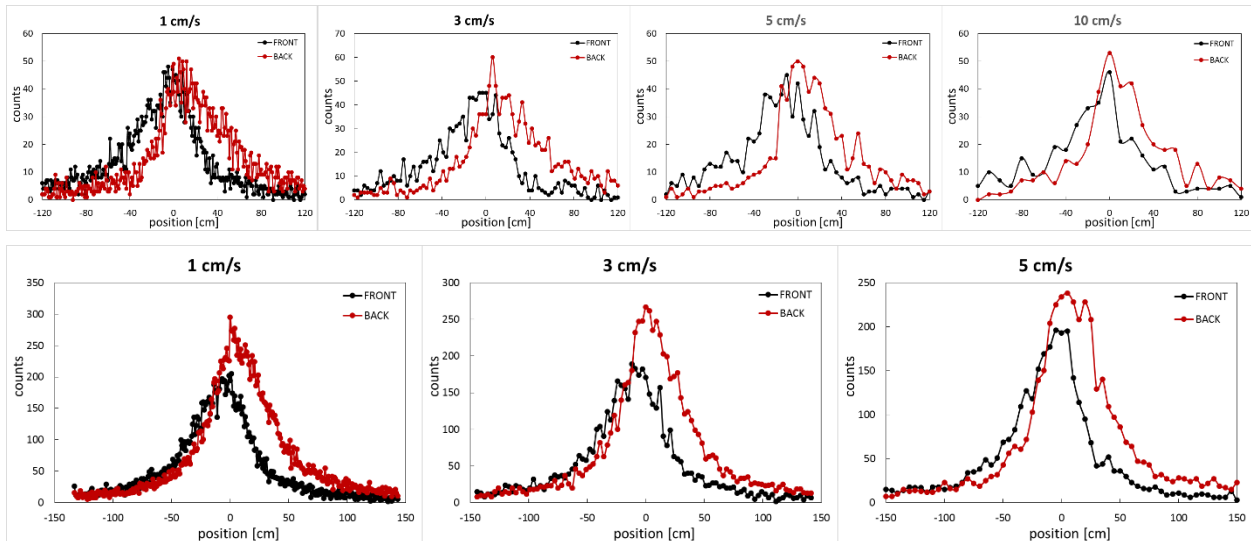


Figure 13. Source moving toward the front face of HDND positioned sideways with respect to the source; (top)  $^{252}\text{Cf}$  speed increased from 1 – 10 cm/s; (bottom)  $^{137}\text{Cs}$  speed increased from 1 – 5 cm/s.

Figure 13 illustrates the sensitivity of HDND to direction of motion by the front cell response shifted with respect to the back cell response. The sensitivity is maintained with increasing speed up to 10 cm/s. These measurements illustrate the potential for HDND to be used as a confirmatory measure to track the direction of motion of nuclear material in process. Further results on the HDND process monitoring capability, including use of fixed shielding are summarized in reference 22.

### ***Capability to Determine Pu Content***

The use of a multi-detector configuration with up to three HDND modules was demonstrated in references 21-23 to enable higher neutron detection efficiency and correlated counting capability. The correlated counting provides a unique signature of neutrons originating in nuclear fission and is traditionally used in nuclear safeguards to assay Pu-content.<sup>2,24</sup> To further evaluate HDND suitability for U/TRU ingot measurements using correlated counting, two HDND modules were tested at Idaho National Laboratory's (INL) Zero Power Physics Reactor (ZPPR) facility.<sup>23</sup> The measurements involved a range of Pu-U-Mo (PUMH) plates (Table 3) with the maximum number of plates (10) corresponding to nearly 2.3 kg of Pu, which provides an opportunity to characterize HDND using materials with Pu mass in the range expected for U/TRU ingot. ZPPR measurements also included PUMH plate configurations with added  $^{154}\text{Eu}$  sources to evaluate effects of increased gamma-ray doses (two  $^{154}\text{Eu}$  sources were used with an estimated dose rate of ~1 R/h at the detector-face). Additionally, measurements with PUMH plates with added  $^{252}\text{Cf}$  source were performed to evaluate effects of  $^{244}\text{Cm}$  present in realistic U/TRU ingot.

Table 3. Characteristics of PUMH plates used in the HDND measurement campaign.

Plate types	PUMH
Material type	Pu-U-Mo
Dimensions (inches)	1/4x2x6
Pu mass (g)	226.36
U mass (g)	422.3
Pu240 %	26 % (RG)

The two HDND modules were set-up facing each other, separated by 14 cm as shown in Figure 14. Each of the modules had 1 mm Sn foil on the front face to reduce the sensitivity to gamma-rays, while maintaining the neutron detection efficiency. The PUMH plates were enclosed in a stainless steel can and were positioned vertically, parallel to the HDND detector front faces. The optimum HV setting was established prior to the start of the PUMH plate measurements to accommodate the entire range of materials available in the ZPPR measurement campaign. The optimum HV setting for this campaign corresponded to 925 V.<sup>23</sup>

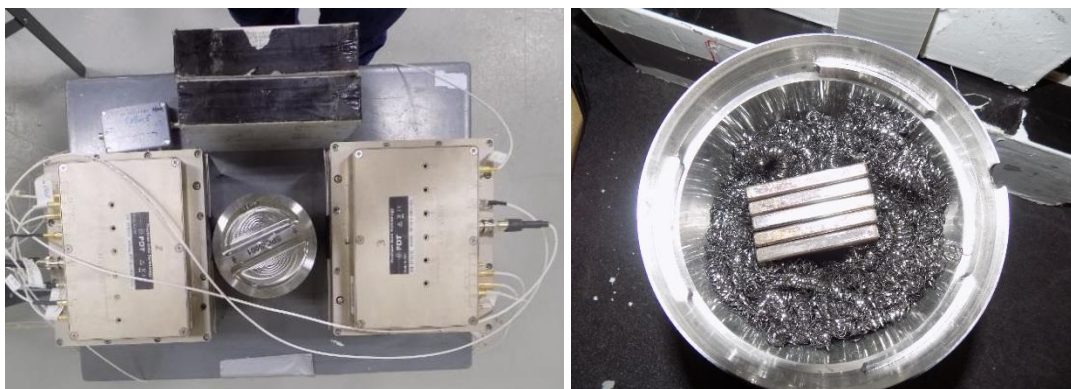


Figure 14. Photographs of HDND set-up during the ZPPR measurements (left) and PUMH plates used inside the stainless steel can (right).

As stated earlier, the measurements provided an opportunity to test HDND for the range of Pu masses representative of U/TRU ingots. However, realistic ingots will include the  $^{244}\text{Cm}$  contribution, which will significantly affect the neutron measurements, as well as high gamma dose rate. To perform an initial evaluation of this contribution and its effects on HDND measurements, configurations with 3 and 5 PUMH plates were repeated with an added pair of  $^{154}\text{Eu}$  sources along with a  $^{252}\text{Cf}$  source. In case of 3 PUMH plates, a strong  $^{252}\text{Cf}$  source was used

(89,135 n/s emission rate), while measurements with 5 PUMH plates included weaker  $^{252}\text{Cf}$  source (75 n/s emission rate). To evaluate the HDND correlated counting performance the Singles, correlated neutron pairs (Doubles) and correlated neutron triplets (Triples) were extracted assuming predelay of 2  $\mu\text{s}$  and gate of 64  $\mu\text{s}$ , which are the detector specific parameters used in correlated neutron counting.<sup>2,25</sup> The measured Singles, Doubles and Triples are summarized in Figure 15.

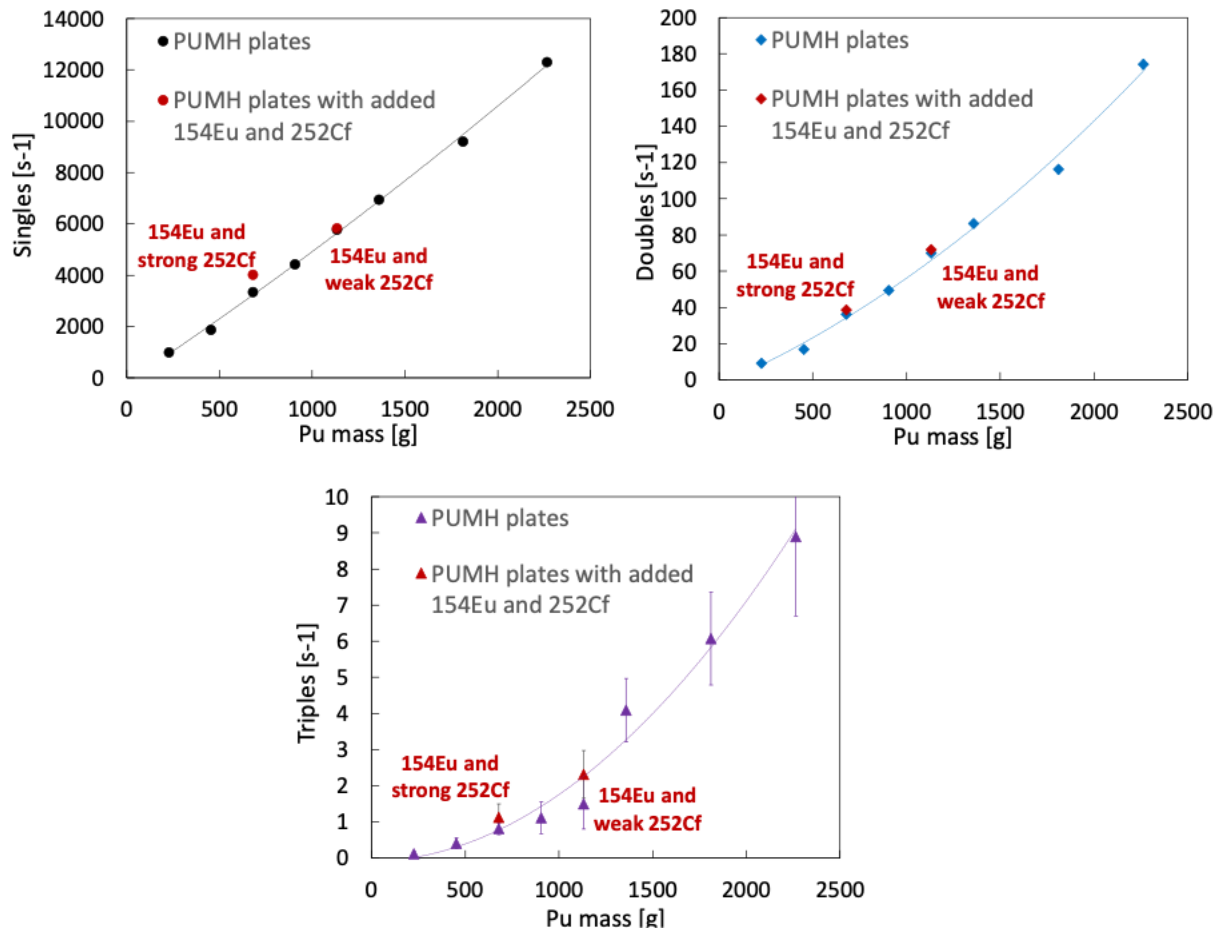


Figure 15. Two HDND pod measured Singles, Doubles and Triples count rates as a function of Pu mass for series of 1 – 10 PUMH plates (note, measurements with 7 and 9 plates were not performed).

Figure 15 illustrates the HDND capability to perform coincidence (Doubles) and even multiplicity (Triples) counting, which is a remarkable result, given only part of cells (approximately one half) were functional. Note that following the installation at ZPPR, a likely power surge issue caused failure of several amplifiers across all the detector cells. A very good performance in coincidence counting is illustrated by low uncertainties and a smooth dependence of Doubles on Pu mass. Triples count rates are very low and exhibit much higher uncertainty, which is to be expected in such a low neutron detection efficiency configuration (i.e. using only half of functional cells in two HDND modules). Nevertheless, the measurement demonstrates the capability to perform multiplicity counting (Triples) for high mass Pu items. Assuming fully functional configuration

(all cells) and all three HDND modules, further reduction of Triples uncertainty can be expected, likely to the point where they could provide an additional feasible observable that could be used to characterize the U/TRU material.

The red data points in Figure 15 correspond to measurements with added  $^{154}\text{Eu}$  and  $^{252}\text{Cf}$  sources, to simulate the effects of increased gamma dose rate and spontaneous fission contribution from  $^{244}\text{Cm}$ . It can be seen that the measurement with added sources results in slightly increased Singles and Doubles count rate, while the effect on Triples is negligible within uncertainty. The addition of  $^{252}\text{Cf}$  is expected to increase both Singles as well as Doubles count rates due to its own spontaneous fission as well as through inducing fissions in the item. For a realistic U/TRU ingot, the magnitude of this effect will depend on the actual concentration of  $^{244}\text{Cm}$ , however, the contribution of  $^{244}\text{Cm}$  will largely cancel out in Doubles-to-Singles ratio as discussed further.

To fully demonstrate HDND capability to extract Pu content, additional analysis methods, outlined in reference 22 were evaluated. The Doubles-to-Singles (D/S) ratio provides a measure of multiplication inside the item and is, therefore, sensitive to Pu content.<sup>26</sup> The D/S ratio for both HDND detectors, normalized to 1 to reflect multiplication (M), is shown in Figure 16 (left). The measurement times for each configuration of PUMH plates (i.e. Pu mass) corresponded to 1000 s. Based on the measurement uncertainty of the D/S for the two-HDND system, the results demonstrate the capability of a pair of HDND modules to measure multiplication with an overall measurement uncertainty of <5% on the D/S ratio in 1000 s. Figure 16 (right) illustrates the potential capability of a single HDND module to extract multiplication despite the half of the full efficiency performance caused by the amplifier failure mentioned above.

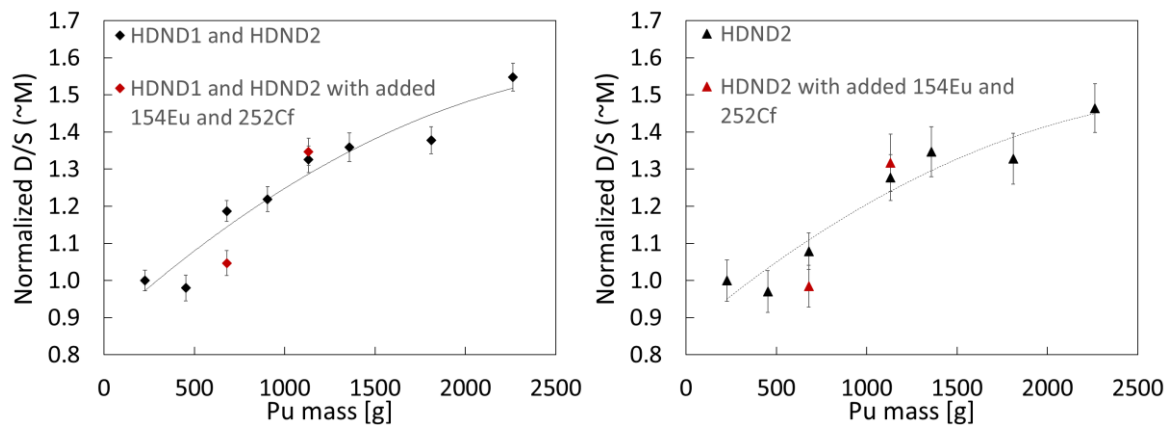


Figure 16. Normalized Doubles-to-Singles ratio for two HDND modules (left) and single HDND module (right).

The red data points in Figure 15 represent measurements with 3 and 5 PUMH plates and added  $^{154}\text{Eu}$  and  $^{252}\text{Cf}$  sources. The D/S ratio for  $^{252}\text{Cf}$  (and similarly  $^{244}\text{Cm}$ ) is expected to be a constant, proportional to detection efficiency and largely independent of  $^{252}\text{Cf}$  mass.<sup>25</sup> The mass of  $^{244}\text{Cm}$  in U/TRU will generally change from batch to batch and result in variable contribution to Singles and Doubles. However, the dependence on  $^{244}\text{Cm}$  mass will largely cancel out in D/S ratio. The D/S ratio should, therefore, remain a strong indicator of multiplication within U/TRU and provide

a good measure of Pu content. Note that induced fissions in Pu will form the dominant contribution to U/TRU ingot multiplication, due to the low expected U:Pu ratio (<1) and ~1% <sup>235</sup>U enrichment.

### ***Hardware Considerations - Miniature HDND***

In the case of an electrochemical processing facility, the majority of processes will be conducted in hot cells filled with an inert atmosphere such as Argon gas and will involve a harsh radiation environment with often very high temperatures due to the nature of process equipment (temperatures on the surface of electro-refiner can reach 100-200 °C). Furthermore, activities inside the hot cell will require use of remote tools and be limited in space, as well as electrical connections and maintenance capabilities. Instrument design will need to be sturdy and support the use of remote tools for any manipulation or maintenance needs. Such an environment and operating conditions pose further challenges to instrumentation hardware.

To this end, a follow-up development was pursued to optimize the HDND neutron detection technology for practical constraints of electrochemical processing applications. A miniature version of HDND instrument (miniHDND) was developed, which introduces a smaller and more flexible and versatile neutron detection instrument that could be placed near process equipment, in confined locations. This would expand HDND use for process monitoring.

The miniHDND represents a compact version of HDND with updates for hot-cell operations while preserving the key HDND detection characteristics. The instrument is designed with a metal enclosure and sufficiently small footprint to simplify handling. It includes three detection cells to maintain its direction of motion capability with the middle cell not coated with boron and therefore serving as a gamma monitor. Due to its compact dimension and reduced efficiency, the miniHDND is foreseen as a process monitoring instrument using neutron and gamma counting. To assure miniHDND compatibility with the hot cell operations and environment, a removable electronics junction box was developed (Figure 17). The key focus was to accommodate high radiation, high temperatures, inert gas as well as handling and maintenance using manipulators. The junction box includes three PDT fast amplifiers with modifications to accommodate high radiation and Argon atmosphere, and it is fully removable to facilitate replacement in case of malfunction or failure. The design includes guide pins to assist with its insertion/removal and a fully sealed detector body to allow for junction box removal without exposure of detector internal components. Such design should assure practical applicability of miniHDND in electrochemical processing environments by improving remote handling experience and simplifying component replacement requirements.

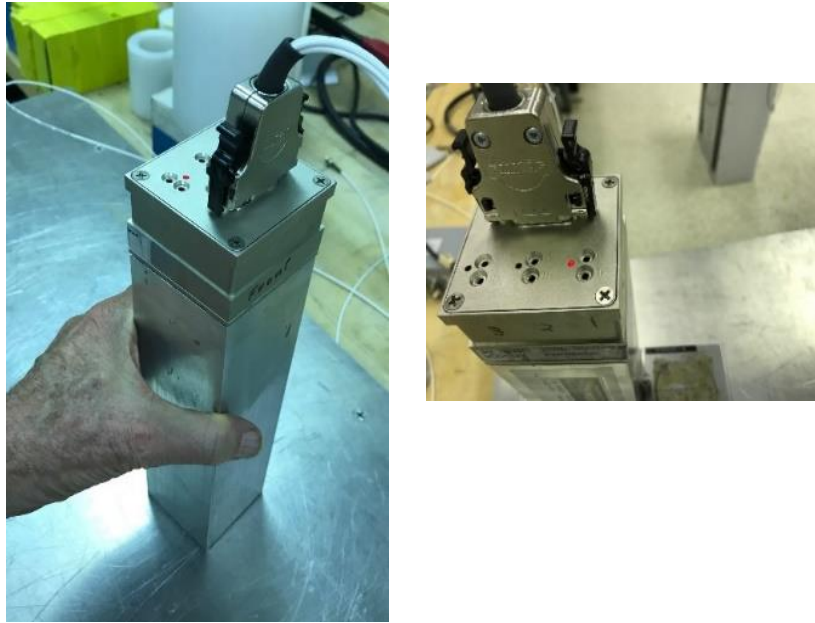


Figure 17. The miniHDND detector with the custom wiring release connector (left) and the 3 LED indicator lights (right). The overall length of the detector is 29 cm.

## Summary and Recommendations for Implementation

Gamma-ray and neutron counting signatures will provide valuable information for safeguards throughout an electrochemical processing facility. Electrochemical processing applications will present unique and new challenges to NDA technologies because of non-standard types and forms of nuclear materials as well as facility environments and layouts. These challenges have driven development and evaluation of the SOFIA microcalorimeter gamma spectrometer and the High Dose Neutron Detector.

The SOFIA gamma spectrometer was designed for deployment to nuclear facilities and analytical laboratories with a compact, low-power cryostat system that can be operated in nearly any facility worldwide. A 256-pixel microwave-multiplexed transition-edge sensor microcalorimeter array enables high-throughput measurements of the 30-210 keV energy range with 5-8 times better energy resolution than planar HPGe in order to resolve the highest-intensity gamma rays from the most important actinides in the presence of intense fission product activity. SOFIA can significantly improve the probability of detection of changes in actinide content of input spent nuclear fuel, ER salt, and U/TRU products compared to planar HPGe for a given number of counts or a given measurement time. The passive, nondestructive nature of ultra-high-resolution microcalorimeter gamma spectroscopy enables implementation in-line with process equipment or sampling loops. For example, SOFIA could potentially be located at the end of a long, shielded collimator that extends into a hot cell where an electrorefiner is operated. Implemented in an on-site analytical laboratory, SOFIA could enable precise measurement of the isotopic composition

of process samples in a much more rapid and cost-effective manner than destructive analysis. Daily nondestructive measurements to determine changes in key isotopic ratios with 1% precision for input fuel, ER salt, and U/TRU product are feasible with the current instrument. The scalable instrumentation architecture demonstrated in SOFIA has great potential to enable future microcalorimeter instruments with yet higher detection efficiency and count rate capability, such as the 500-pixel-scale instrument now being commissioned for permanent installation at the Idaho National Laboratory analytical laboratory.

Key requirements for neutron detection technology will include the capability to perform reliable neutron counting over a broad dynamic range in high gamma backgrounds as well as the capability to accommodate high neutron count rates. For use in a hot cell, the instrument must be compatible with remote handling and limited access for maintenance. To address these issues, LANL has developed an advanced neutron detection instrument, HDND, which has been demonstrated to provide:

- High neutron count rate capability and broad dynamic range;<sup>21</sup>
- Low and tunable gamma-ray sensitivity;<sup>21</sup>
- Dual detection mode capability (neutron and gamma detection);<sup>21,27</sup>
- Direction of motion measurement capability (from multi-plate design);<sup>22</sup>
- Sufficient neutron detection efficiency for correlated counting (in configurations with 2 or more HDND modules).<sup>21,22,23</sup>

In particular, the U/TRU ingot measurement capability was demonstrated using a range of Pu-U-Mo (PUMH) plates of up to 2.3 kg of Pu. These results demonstrated the capability of a system of two HDND modules to measure multiplication via the D/S ratio technique with an overall measurement uncertainty of <5% on the D/S ratio in 1000s. Note that the HDND was operated at only half of the full efficiency for the D/S measurements in this report. A system of three fully functional HDND units would, therefore, provide a further improvement in the overall measurement uncertainty. Prior multiplication versus Pu-mass calibration using MCNP would be required to extract U/TRU ingot Pu-content from the HDND D/S measurement. Also, the current work demonstrated that HDND is capable of tolerating an increase in gamma dose rate by almost two orders of magnitude (up to 800 R/hr) with only ~30% reduction in neutron detection efficiency. This is an essential result confirming the HDND capability to perform neutron measurements in a high gamma-dose environment without significant gamma interference. Finally, the HDND process monitoring capability was demonstrated using moving neutron and gamma sources. Moving source speeds up to 10 cm/s were evaluated with a clearly distinguishable signature of the direction of motion in the HDND signal. This will provide another valuable capability for use of HDND to monitor nuclear material movements through the electrochemical process.

Hardware aspects related to remote handling and hot-cell use were also addressed in a dedicated miniature HDND (miniHDND) development, which was fully tailored to accommodate limited maintenance capabilities, confined areas and use of manipulators. The miniHDND has an exterior metal body with a removable junction box to simplify component replacements in case of amplifier failure. The miniHDND could be important for in-cell measurements that confirm that vessels are empty at the time of a material balance.

By leveraging these advanced nondestructive gamma ray and neutron measurement technologies, the development of a robust and economic safeguards approach will be an important enabling capability for the next generation of nuclear energy.

## **Keywords**

Nondestructive assay, nuclear safeguards, gamma ray spectroscopy, microcalorimetry, correlated neutron counting, boron-lined detector

## **Acknowledgements**

This work is supported by the United States Department of Energy, Office of Nuclear Energy, Material Protection Accounting and Control Technologies (MPACT) program and Nuclear Energy University Program (NEUP). The microcalorimeter development team includes Michael Yoho, Katrina Koehler, Matthew Carpenter, Aidan Tollefson, and Chandler Smith of Los Alamos National Laboratory; Nathan Ortiz, Johnathan Gard, and Abigail Wessels of the University of Colorado; and Douglas Bennett, Gene Hilton, John A.B. Mates, Carl Reintsema, Daniel Schmidt, Daniel Swetz, and Leila Vale of the National Institute of Standards and Technology. Spent fuel samples were provided by David Meier and Bruce Pierson of Pacific Northwest National Laboratory. Electrorefiner salt samples were provided by Jeff Sanders of Idaho National Laboratory. The HDND authors would like to acknowledge the excellent support during the field test measurements by Robby Weinmann-Smith, who coordinated the campaign for LANL and on-site INL team led by Jeff Sanders.

## **Author Biographies**

Mark Croce is a Scientist in the Safeguards Science and Technology group in the Nuclear Engineering and Nonproliferation division of Los Alamos National Laboratory. He has over 15 years of experience in the development of cryogenic detector systems and novel instrumentation for nondestructive nuclear material analysis. He holds a bachelor's degree in physics from the University of California, Santa Barbara.

Daniela Henzlova is a Scientist at the Safeguards Science and Technology Group in Los Alamos National Laboratory with 20 years of experience in nuclear physics measurements and instrumentation. She holds a PhD in Nuclear Engineering from the Czech Technical University in Prague.

Howard Menlove received his PhD in Nuclear Engineering from Stanford University in 1965, and for more than 50 years, he has worked in the Nuclear Safeguards and Nonproliferation Program at the Los Alamos National Laboratory. He was awarded the Los Alamos Fellow position in 1980 and the Los Alamos Medal in 2018. He developed many of the neutron measurement systems that are in worldwide use by the IAEA and international inspectorates.

Daniel Becker is a Research Associate at the University of Colorado and a member of the NIST Quantum Sensors Group. He has 14 years of experience working with cryogenic detector systems,

covering both the development of new scientific instruments and new data analysis techniques and algorithms. He holds a PhD in Physics from the University of Colorado.

Joel Ullom is a Lecturer in the Department of Physics at the University of Colorado Boulder and the leader of the NIST Quantum Sensors Group. He has worked in the field of cryogenic electronics since 1994 and has led the development of spectrometers for materials analysis based on multiplexed arrays of transition-edge sensors. He holds a PhD in Physics from Harvard University.

## References

1. Cipiti, B. B., Browne, M., and Reim, M. 2021. The MPACT 2020 Milestone: Safeguards and Security by Design of Future Nuclear Fuel Cycle Facilities, *J. Nucl. Mater. Manage*, Vol. X, No. X.
2. Reilly, D. et al. 1991. Passive nondestructive assay of nuclear materials; *Los Alamos National Laboratory Report*, LA-UR-90732.
3. Hoover A. S. et al. 2014. Uncertainty of plutonium isotopic measurements with microcalorimeter and high-purity germanium detectors. *IEEE Trans. on Nucl. Sci.*, 61: 2365-2372.
4. Bacrania, M. K. et al. 2009. Large-area microcalorimeter detectors for ultrahigh resolution x-ray and gamma-ray spectroscopy, *IEEE Trans. Nucl. Sci.*, 2299–2302.
5. Mates, J. A. B. et al., 2017. Simultaneous readout of 128 X-ray and gamma-ray transition-edge microcalorimeters using microwave SQUID multiplexing, *Appl. Phys. Lett.* 111, 062601.
6. Bennett, D. A. et al. 2015. Integration of TES Microcalorimeters with Microwave SQUID Multiplexed Readout, *IEEE Transactions on Applied Superconductivity*, 25: 1-5.
7. Gard J. D. et al. 2018. A Scalable Readout for Microwave SQUID Multiplexing of Transition-Edge Sensors, *Journal of Low Temperature Physics*, 193: 485-497.
8. Yoho, M. et al. 2020. Automated co-adding and energy calibration of large array microcalorimeter data with zero sample knowledge, *Nuclear Instruments and Methods in Physics Research Section A*.
9. Becker. D. T. et al. 2019. Advances in Analysis of Microcalorimeter Gamma-Ray Spectra, *IEEE Trans. on Nucl. Sci.*
10. Harris, N.C. et al. 2021. University Research to Support the MPACT 2020 Milestone, NEUP Development Paper, *J. Nucl. Mater. Manage*, Vol. X, No. X.
11. ROACH2, 2020, available at <https://www.digicom.org/roach-board.html>.
12. Sampson, T., Nelson, G., and Kelley, T. 1989. FRAM: A versatile code for analyzing the isotopic composition of plutonium from gamma-ray pulse height spectra Los Alamos Nat. Lab., LA-II720-MS, Los Alamos National Laboratory.
13. Yoho, M. et al. 2020. Improved Plutonium and Americium Photon Branching Ratios from Microcalorimeter Gamma Spectroscopy, *Nuclear Instruments and Methods in Physics Research Section A*.
14. Arrigo, L.M. et al. 2009. FY 2009 Progress: Process Monitoring Technology Demonstration at PNNL, PNNL-19136, Pacific Northwest National Laboratory.

15. Montgomery, R. et al., "Post-Irradiation Examinations of High Burnup PWR Rods", WM2018 Conference Proceedings, OSTI 1480633, 2018.
16. Henzlova, D., Menlove, H. O. 2016. Report on MPACT Deliverable M4FT-16LA0406034 (complete MCNP optimization work), *Los Alamos National Laboratory Report*, LA-UR-16-20189.
17. Brown, W.K., Jensen, T.H. 1964. On Electron Drift Velocities in Mixtures of Noble Gases and 'Moderator' Gases, *Nuclear Instruments and Methods* 27, 259-265.
18. Kopp, M. K., et al. 1982. New Gas Mixture Improves Performance of <sup>3</sup>He Neutron Counters, *Nuclear Instruments and Methods* 201, 395-401.
19. Kusano, H., et al. 2008. Measurements of Electron Drift Velocity in <sup>3</sup>He Gas, *Japanese Journal of Applied Physics* Vol. 47, No. 8, 6475-6477.
20. Henzlova, D., and Menlove, H.O. 2015. High-Dose Neutron Detector Development, *Los Alamos National Laboratory Report*, LA-UR-15-27500.
21. Henzlova, D., and Menlove, H. O. 2017. Report on operational test of High Dose Neutron Detector, *Los Alamos National Laboratory Report*, LA-UR-17-29204.
22. Henzlova, D., and Menlove, H. O. 2018. Final Report on High Dose Neutron Detector for FY18, *Los Alamos National Laboratory Report*, LA-UR-18-29899.
23. Henzlova, D., Menlove, H. O., Weinmann-Smith, R. 2019. Report on MPACT Deliverable M3FT-19LA040106026 (Continuation of HDND deployment at INL), *Los Alamos National Laboratory Report*, LA-UR-19-31511.
24. Menlove, H. O. 1987. The Role of Neutrons in Safeguards, *JNMM* XV(4), 83-87.
25. Ensslin N., Harker W.C., Krick M.S., Langner D.G., Pickrell M.M., Stewart J.E.. 1998. Application guide to neutron multiplicity counting, *Los Alamos National Laboratory Manual*, LA-13422-M.
26. Menlove, H. O., Abedin-Zadeh, R., Zhu, R. 1989. The Analysis of Neutron Coincidence Data to Verify Both Spontaneous Fission and Fissionable Isotopes, *Los Alamos National Laboratory Report*, LA-11639-MS.
27. Henzlova, D., Menlove, H. O., Sanders, J., Williams, A. 2018. Report on MPACT Deliverable M2FT-18LA040106031 (HDND field test with mixed neutron gamma field), *Los Alamos National Laboratory Report*, LA-UR-18-24696.